Generation of Coherent Zone Boundary Phonons by Impulsive Excitation of Molecules

M. Gühr, M. Bargheer, and N. Schwentner

Institut für Experimentalphysik, Freie Universität Berlin, Arnimallee 14, 14195 Berlin, Germany

(Received 27 May 2003; published 21 August 2003)

A coherent zone boundary phonon (ZBP) of solid Kr ($f_m = 1.54$ THz) is observed in ultrafast pump-probe spectra of I_2 guest molecules in a Kr crystal. Its phase is stable for at least 10 ps. The femtosecond pump pulse induces an electronic transition in I_2. The resulting expansion of the guest's electronic cloud impulsively excites phonons in the host. Detection at the impurity after some picoseconds selects the ZBP due to its low group velocity. A ZBP amplitude of 0.02 Å is estimated.

DOI: 10.1103/PhysRevLett.91.085504 PACS numbers: 63.20.Mt, 31.70.Dk, 31.70.Hq

Electronic excitation of an atom or molecule changes the shape and extension of its electronic wave function. If the atom or molecule is embedded in a host, the electronic excitation will enforce a change of the equilibrium position of host atoms in the vicinity of the excited guest. After an impulsive excitation, the atoms can be expected to oscillate around their new equilibrium position. This mechanism is known as displacive excitation of coherent phonons (DECP) [1,2]. This process was studied extensively for an electronic excitation of pure conducting and semiconducting materials by monitoring a modulation of the reflectivity. Exclusively zone center optical phonons, predominantly with A_1 symmetry, were excited coherently [1]. We investigate electronic excitation of a diatomic molecule (I_2) embedded in the bulk of rare gas polycrystalline films. The fcc lattice of rare gas crystals has only acoustic phonons with very well characterized longitudinal and transversal phonon branches [3]. Our investigations result in a selection of phonons different from Refs. [1,2]. We show that very monochromatic zone boundary phonons (ZBP) are created, which remain coherent in the vicinity of the excited molecule for a long time of more than 10 ps (about 15 ZBP periods). Zone center phonons propagate with the velocity of sound while the dispersion leads to a lower velocity at the zone boundary, where phonons exhibit a group velocity v_g approaching zero. In fact, the small group velocity is essential for preserving the phonon amplitude in the vicinity of the molecule for the observed long time.

A number of mechanisms have been employed in the past two decades in the formation of coherent vibrations. Screening of space-charge fields [1] cannot be relevant in our case. Impulsive stimulated Raman scattering was used to prepare coherent vibrations in dissolved molecules [4]. While internal coordinates of the dissolved molecules were driven in these studies, we show that in our case host phonons are coherently excited by the DECP process initiated by excited molecules. The breathing modes observed in F center dynamics seem to be rather closely related to our topic; however, they represent once more a superposition of zone center optical phonons [5] with A_1 symmetry. The coupling of electronically excited atoms [6] as well as diatomic molecules such as I_2 [7–10], Cl_2 [11], and NO [12] to a lattice was treated theoretically by several groups. The simulations reveal the generation of shock waves which propagate with high velocity along the (110) nearest neighbor rows of the host lattice away from the center [7]. Coupling to a superposition of modes within the host phonon spectrum with a beating and loss of pronounced coherence within a few picoseconds is predicted [8–11]. Our observation of long lived coherent ZBP which are generated by this electronic excitation is not reproduced in the simulations and requires a new analysis.

Samples of 30 μm thick clear crack-free films of Kr doped with I_2 in a ratio of 1000:1 were prepared [13] and investigated at 20 K. Two laser pulses with a FWHM of less than 40 fs which are independently tunable in the visible spectral range were generated by two noncollinear optical parametric amplifiers pumped by a commercial Ti:sapphire laser [14]. In addition, the frequency doubled fundamental of the Ti:sapphire laser with a wavelength of 387.5 nm and a FWHM of 120 fs was used. One pulse generates a vibrational wave packet in the A or B state depending on wavelength (pump in Fig. 1). The second pulse (probe in Fig. 1) excites the wave packet to the β or E state. Fluorescence from the lowest ionic state D' [16] was recorded at 408 nm. The intensity of laser induced fluorescence versus the time delay between both pulses is shown in Fig. 2. It displays the relevant wave packet dynamics.

Spectra for B and A state excitation were recorded in several investigations and analyzed with respect to the host induced modifications of I_2 potential energy surfaces [13], vibrational relaxation [17], predissociation [16], and depolarization [18]. The strongly modulated part in the time trace [Fig. 2(a)] decays within about 3 ps and represents the vibrational oscillation in the B state with a round trip time of 420 fs corresponding to a frequency of 2.5 THz (84 cm^{-1}). The width of 10 cm^{-1} in a Fourier transformation reflects the anharmonicity within the wave packet which is composed of about 5 to 10 vibrational levels. The wave packet falls below the probe window (located at an I-I distance of 0.36 Å in Fig. 1

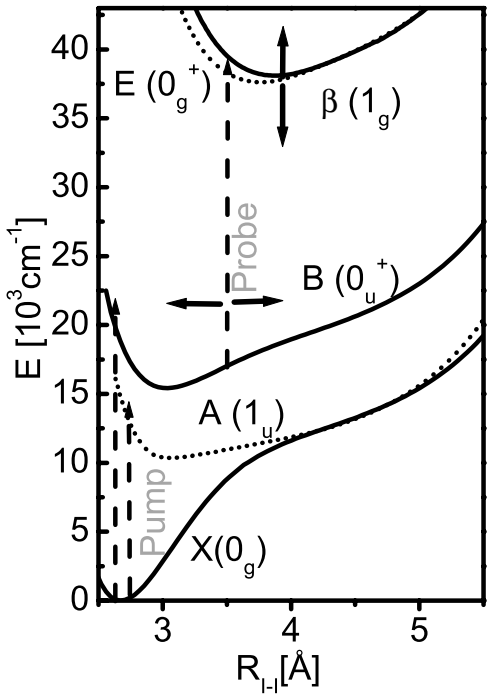

FIG. 1. Potential energy scheme of I_2:Kr [15]. B (solid line) and A (dashed line) are covalent states, β (dashed line) and E (solid line) are ionic states. Population from ground state X is pumped to covalent states (dashed arrows) and probed to ionic states (B to E with dashed arrow) after some time t. If the phonon shifts the ionic state energy up and down (vertical solid arrows), the probe window position R is shifted (horizontal arrow).

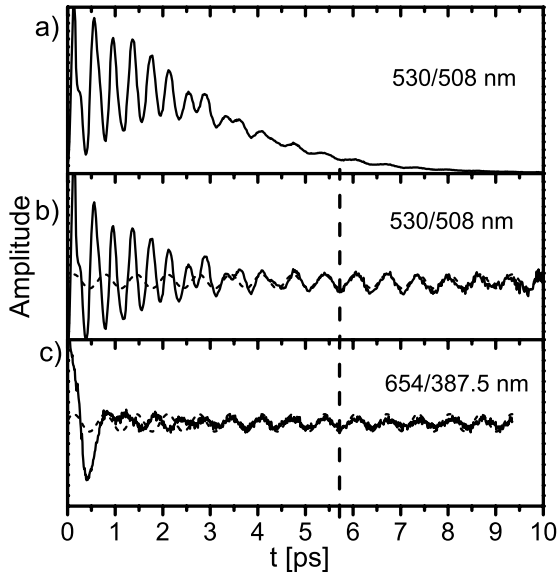

FIG. 2. (a) Experimental pump-probe spectrum with $\lambda_{\text{pump}} = 530$ nm ($B \leftarrow X$), $\lambda_{\text{probe}} = 508$ nm ($E \leftarrow B$), and fluorescence recorded at 408 nm. (b) Solid line: same spectrum as in (a) but normalized to mean value. After about 4 ps the spectrum is sinusoidal with a period of $T = 650$ fs (dashed line). (c) Normalized spectrum (solid line) for excitation of the A state ($\lambda_{\text{pump}} = 654$ nm) and probing to β ($\lambda_{\text{probe}} = 387.5$ nm), with same sin curve as in (b) (dashed line). The phase of the 650 fs modulation relative to $t = 0$ fs is the same in all plots (dashed vertical line at 5.7 ps).

for the chosen probe wavelength of 508 nm) due to vibrational relaxation and therefore the averaged intensity decays monotonically. A further periodic modulation with a different frequency of $f_m = 1.54$ THz (650 fs or 51.5 cm^{-1}) is superimposed on the decaying signal at later times between 3 and 12 ps. It is hardly visible in Fig. 2(a) due to the strong decay of the mean value. However, it can be enhanced by normalization to the time averaged signal.

The resulting Fig. 2(b) shows, from 4 ps on, exclusively the frequency f_m with an essentially constant amplitude until it is lost in the scatter of the mean value around 12 ps. This signal with the 1.54 THz frequency represents the relevant feature here, which will be ascribed to the coherent host phonon. The same f_m is observed for different B state vibrational wave packet periods resulting from a variation of excitation energies in the anharmonic well. In a previous investigation the 1.54 THz oscillation was observed [8] without recognizing its independence on B state dynamics. It was therefore mistaken as a driven oscillation. This independence on I_2 vibrational dynamics is confirmed by the fact that f_m is observed also for A state excitation, where the molecular vibration has an entirely different period [Fig. 2(c)]. The A state wave packet decays once more in 3 ps. From 3 ps on, a modulation with constant amplitude and the very same frequency f_m as for the B state is observed. The probe wavelength in Fig. 2(c) was tuned to 387.5 nm in order to probe the A state population up to the β state (Fig. 1). The fluorescence wavelength selection [16] ensures that f_m does not originate from another I_2 potential energy surface. In addition, f_m cannot be caused by vibrational wave packets in the electronic ground state from impulsive stimulated Raman scattering because the frequency would be a factor of 4 higher than f_m. Finally, not only is f_m the same for Figs. 2(b) and 2(c), even the phase relative to $t = 0$ is the same as indicated by the vertical line at 5.7 ps. This identical phase confirms that the mode f_m has to be excited impulsively by the pump pulse at $t = 0$. Therefore, we can trace back the time evolution of f_m and, indeed, we find for all spectra the same phase at $t = 0$ as shown by the dashed oscillation in Figs. 2(b) and 2(c). Within the reliability of the extrapolation it corresponds to a $\cos(2\pi f_m t)$ function which is consistent with the DECP mechanism [1].

The Fourier transform of the solid line in Fig. 2(b) is displayed in Fig. 3(b) and shows a sharp single line at the expected frequency of $f_m = 1.54$ THz beside the molecular vibration at 2.5 THz which is not included. The line width FWHM of 0.1 THz or 6% of f_m corresponds essentially to the inverse of the time window of observation and represents, therefore, only an upper limit. For comparison, we represent the phonon dispersion curve of solid Kr along [100] from neutron scattering in Fig. 3(a).

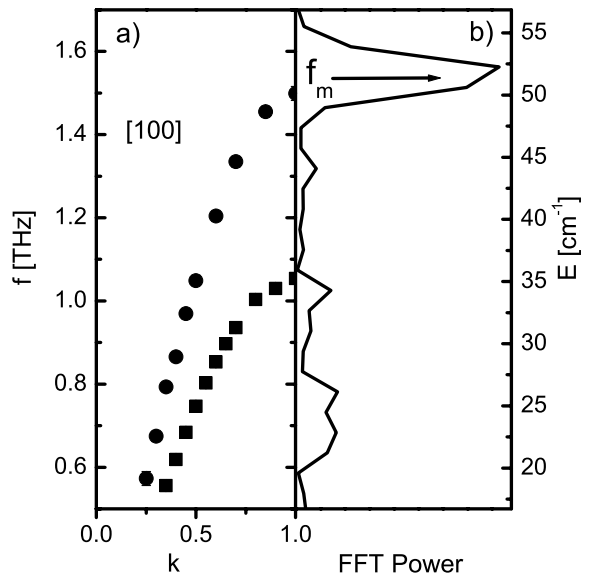

FIG. 3. (a) Phonon dispersion relation for solid Kr at 10 K in the [100] direction showing transversal (circles) and longitudinal (squares) phonons [3]. (b) Fourier transform of spectrum in Fig. 2(b) shows ZBP with $f_m = 1.54$ THz.

The data are taken from Ref. [3]. Obviously, f_m represents the upper zone boundary phonon energy within the error bars of both experiments.

We suggest an explanation for the generation of ZBPs based on the DECP mechanism. The I_2 molecule replaces two Kr atoms of the fcc lattice in a substitutional way which leads in the (111) plane to the geometry sketched in Fig. 4(b). The three cap atoms on both ends of the I_2 molecule are pushed outwards in a bond extension of the vibrating molecule, while the atoms at the belt are forced to move inward. Therefore, the cage atoms in the (111) plane are strongly coupled to the molecular vibrational wave packet [8,11,17] and not suited to detect the DECP contribution. The pairs of atoms 1,2 in the (100) plane [Fig. 4(a)] and their mirror image are decoupled from the molecular vibration because the I atoms move like a piston parallel to the wall formed by these atoms. This intuitive picture is confirmed by the contours of minimal potential energy in the A state for two I_2 bond lengths of 0.264 and 0.5 Å [Fig. 4(c)]. The belt contour moves inward and the cap outward for the bond extension. However, the contour at the position of atoms 1 and 2, which are equivalent, remains essentially unchanged. The contours are calculated from a summation of pair potentials given in [9], using the diatomics in molecules diagonalization [10]. With respect to the X state contour, the A state contours at 1 and 2 are shifted outwards by about 0.15 Å corresponding to 3% of the I-Kr distance [Fig. 4(c)]. Thus, the electronic transition from X to A results in an outward push at $t = 0$ of the Kr atoms in positions 1 and 2 and they are going to oscillate around the new equilibrium position which is enlarged by about 3%. The B state yields contours similar to A and both transitions provide the scenario for the DECP mechanism

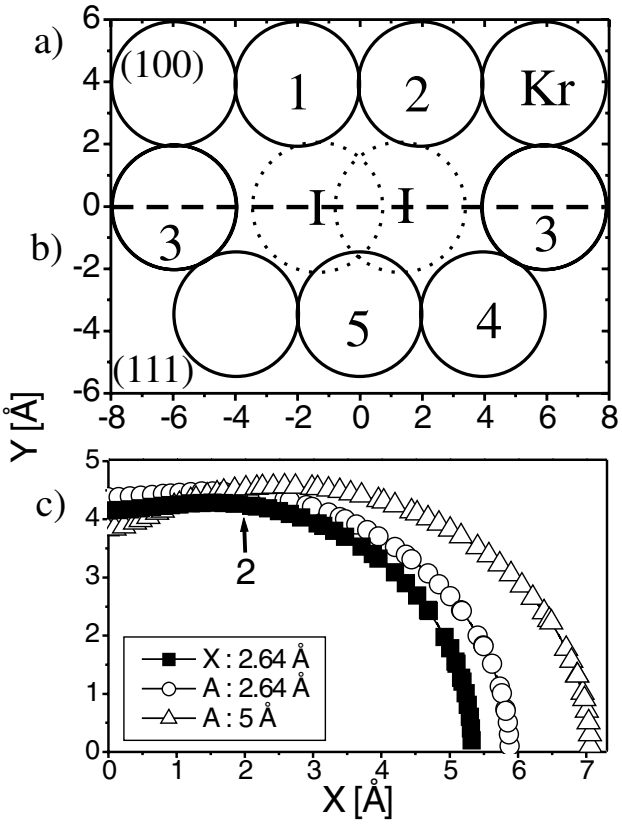

FIG. 4. (a) and (b) should be mirror imaged at the dashed line to reveal the full symmetry. (a) Geometry in the (100) plane of the fcc Kr lattice doped by I_2. Atoms 1 and 2 are decoupled from the vibrational motion of the molecule. (b) Geometry in the (111) plane. Head on atoms 3 [identical to (100) plane], cap atom 4 and belt atom 5 are strongly coupled to the vibration of I_2. (c) Contours of minimal potential energy for ground state at internuclear distance $R_{I-I} = 2.64$ Å (squares) and the A state at inner (open circles) and outer (open triangles) turning points. The arrow indicates the position of atom 2 in the (100) plane, where the contours are insensitive to bond length.

in combination with atoms 1 and 2. Atoms 1,2 and their mirror images [Fig. 4(a)] drive phonons which propagate in opposite directions with wave vectors k and $-k$. In this way, the wave vector selection rule $\Delta k = 0$ for optical transitions is fulfilled and the displacements preserve the original D_{2n} symmetry of the I_2 site. With respect to the Raman activity of these modes, it is well known that pure rare gas crystals possess only a Raman spectrum of second order. The pairwise excitation of k and $-k$ phonons is analogous to a second order process and the full spectrum of phonons is accessible according to the second order Raman spectrum [19].

Finally, we discuss the detection scheme. The coherent phonons appear as an intensity modulation on the molecular $\beta \leftarrow A$ and $E \leftarrow B$ probe transitions. The valence states A and B are weakly redshifted in the Kr matrix compared to the gas phase by only some hundred wave numbers. The ionic E state is lowered in energy by about 3400 cm^{-1} due to solvation of the dipole in the

polarizable Kr matrix [17]. The solvation energy in the Onsager model scales with the reciprocal third power of the cavity radius, corresponding to the I-Kr distance [20]. An expansion of the cavity lowers the solvation energy and the E state in Fig. 1 goes up in energy. Consequently, the spatial position of the probe window on the $R_{\mathrm{I-I}}$ coordinate moves outwards, because the probe photon energy for optimal sensitivity is given by the difference potentials $\beta - A$ or $E - B$. Thus, the vibrational wave packet is now probed at a higher energy. The decay of the mean signal in Fig. 2(a) originates from the energy relaxation of the wave packet out of the probe window. An expansion of the matrix raises the probe energy position and leads to an intensity decrease. A shrinking brings the probe window closer to the center of the wave packet and enhances the signal intensity. The ground state X of I_2 represents the most compressed configuration according to Fig. 4(c). Excitation to A or B starts an expansion to the new contour. The matrix density as well as the signal intensity should decrease from its maximal value according to $\cos(2\pi f_m t)$, which is in agreement with the extrapolations to $t = 0$ in Figs. 2(b) and 2(c). Using this detection scheme and the confirmation of the phase of the coherent phonons at $t = 0$, we can now estimate the displacement amplitude using the intensity modulation of about 10% [Fig. 2(b)]. The vibrational relaxation rate in the B state has been determined carefully [17] and in the region of the probe window it corresponds to an energy loss of 70 cm^{-1} within one ZBP period. From the intensity decrease in Fig. 2(a) and the energy relaxation data, one obtains an energy modulation of the ionic E state of 40 cm^{-1}. Using these data, the Onsager model [20] predicts a cavity diameter variation of about 0.5% corresponding to a ZBP amplitude of 0.02 Å. This value is consistent with the expected displacements of the new equilibrium configurations in Fig. 4(c). It is large in comparison to typical displacements from the DECP mechanism in semiconductors but lies well below that for very high excitation intensities where anharmonicity and mode coupling come into play [2].

In this detection scheme only phonon amplitudes next to the I_2 guest molecule contribute to the modulation. We briefly discuss assignments of f_m alternative to the ZBP. Typical librational frequencies (resulting from hindered rotation) for CO or HCl in rare gas crystals are smaller than f_m. They scale with the inverse of the rotational constant B_e, and therefore we would expect the librational frequency for I_2 to be much smaller than f_m. The local phonon calculated in [8] does not give the required phase stability. Thus, we remain with the ZBP assignment. The observed linewidth is in accordance with ZBP calculations [21]. Using the dispersion relation and the observed linewidth (Fig. 3), we estimate an upper limit for the spreading of the ZBP of five lattice constants in 10 ps, in accordance with the observed preservation of amplitudes near the impurity. Obviously, ZBPs with their specific property of $v_g \rightarrow 0$ are prone to be recorded in this scheme. The phonons which showed up in several simulations [7] had large group velocities and their amplitudes would be damped by propagation. Thus, the detection scheme provides a purification of the phonon spectrum with strong preference for $v_g = 0$ and zone boundary contributions. We expect that further simulations which are specifically devoted to this scenario are going to reveal these coherent phonons for molecular dopants in matrices for the first time theoretically. They can clarify the peculiar excitation scheme, the distribution of amplitudes in the surrounding, and the specific coherent dynamics with a very weak damping.

We gratefully acknowledge support by the Deutsche Forschungsgemeinschaft (DFG), which made this work possible in the project "Analysis and control of ultrafast photoinduced reactions" (SFB 450) and the very fruitful discussions with Professor V. A. Apkarian and Professor R. B. Gerber.

[1] H. J. Zeiger *et al.*, Phys. Rev. B **45**, 768 (1992).
[2] M. Hase, M. Kitajima, S. I. Nakashima, and K. Mizoguchi, Phys. Rev. Lett. **88**, 067401 (2002).
[3] J. Skalyo, Jr., Y. Endoh, and G. Shirane, Phys. Rev. B **9**, 1797 (1974).
[4] J. Chesnoy and A. Mokhtari, Phys. Rev. A **38**, 3566 (1988).
[5] R. Scholz *et al.*, Phys. Rev. B **56**, 1179 (1997).
[6] A. Goldberg and J. Jortner, J. Chem. Phys. **107**, 8994 (1997).
[7] A. Borrmann and C. C. Martens, J. Chem. Phys. **102**, 1905 (1995).
[8] R. Zadoyan, J. Almy, and V. A. Apkarian, Faraday Discuss. **108**, 255 (1997).
[9] M. Ovchinnikov and V. A. Apkarian, J. Chem. Phys. **105**, 10 312 (1996).
[10] V. S. Batista and D. F. Coker, J. Chem. Phys. **106**, 6923 (1997).
[11] M. Ovchinnikov and V. A. Apkarian, J. Chem. Phys. **108**, 2277 (1998).
[12] S. Jimenez, M. Chergui, G. Rojas-Lorenzo, and J. Rubayo-Soneira, J. Chem. Phys. **114**, 5264 (2001).
[13] M. Bargheer, P. Dietrich, K. Donovang, and N. Schwentner, J. Chem. Phys. **111**, 8556 (1999).
[14] M. Bargheer, J. Pietzner, P. Dietrich, and N. Schwentner, J. Chem. Phys. **115**, 9827 (2001).
[15] V. S. Batista and D. F. Coker (private communication).
[16] M. Gühr, M. Bargheer, P. Dietrich, and N. Schwentner, J. Phys. Chem. A **106**, 12 002 (2002).
[17] M. Bargheer, M. Gühr, P. Dietrich, and N. Schwentner, Phys. Chem. Chem. Phys. **4**, 75 (2002).
[18] M. Bargheer, M. Gühr, and N. Schwentner, J. Chem. Phys. **117**, 5 (2002).
[19] P. A. Fleury, J. M. Worlock, and H. L. Carter, Phys. Rev. Lett. **30**, 591 (1973).
[20] L. Onsager, J. Am. Chem. Soc. **58**, 1486 (1938).
[21] M. L. Klein, J. A. Barker, and T. R. Koehler, Phys. Rev. B **4**, 1983 (1971).